

Influence of terrace widths on Au(111) reconstruction

D. Chauraud, J. Durinck,^{*} M. Drouet, L. Vernisse, J. Bonneville, and C. Coupeau
Institut P', UPR 3346, Centre National de la Recherche Scientifique, Université de Poitiers, France
 (Received 31 March 2017; revised manuscript received 9 June 2017; published 11 July 2017)

The effect of steps on the herringbone pattern appearing at the Au(111) surface is explored. Scanning tunneling microscopy investigations show that the number of alternating fcc and hcp regions decreases with the decreasing width of the terrace, in fair agreement with atomistic simulations. It is demonstrated that the steps locally release the tensile surface stresses, leading to a reorganization of the herringbone pattern.

DOI: [10.1103/PhysRevB.96.045410](https://doi.org/10.1103/PhysRevB.96.045410)

I. INTRODUCTION

The field of surface nanostructuring is booming since the 2000's. The challenge is to confer specific properties or to create templates for further functionalization by deposition of molecules or nanoparticles. The Au(111) surface has been studied extensively since the 1990's. Experimental studies [1–7] have highlighted a typical reconstruction, known as a herringbone or chevronlike pattern. It presents interesting opportunities as pattern for self-organized molecules [8] or metallic clusters [9,10], with technological applications in various domains such as microelectronics and nanocatalysis [11,12]. Scanning tunneling microscopy (STM) observations [1–3] have shown that the reconstruction is characterized by alternating fcc and hcp areas at the topmost layer. The misfit between the surface layer and the bulk is accommodated by Shockley dislocations. These subsurface partial dislocations (SPDs) are mainly lying along the $\langle 112 \rangle$ directions, resulting in an out-of-plane displacement of only 15 pm in gold [3]. Such a dislocation network has been already used to describe (111) surface reconstructions of fcc materials [13–15]. Due to the threefold symmetry of the free surface, the resulting herringbone pattern is a combination of two (over three) oriented SPDs. Many attempts have been made to model the Au(111) reconstruction, as for instance the two-dimensional Frenkel-Kontorova modeling for which the substrate is described by a periodic potential interacting with the surface atoms [1,6,16]. It was thus established that the Au(111) reconstruction is driven by tensile surface stresses [17,18]. Molecular dynamics simulations were also carried out to describe the reconstruction at the atomic level [19,20]. In particular, the influence of external stress on the periodicity of the SPDs has been studied, even if not quantitatively in good agreement with the observations [21].

The free surface of single crystals exhibits vicinal steps at the atomic scale, coming from the slight misorientation of the surface with respect to the low-index crystallographic direction. A previous study has demonstrated that the slip traces resulting from the emergence of moving dislocations at the free surface highly modify the organization of the vicinal steps [22]. Only a few studies are, however, focused on the effect of these atomic steps on the herringbone pattern. STM investigations revealed in particular different herringbone structures on the top or bottom sides of a vicinal step [2,23].

It has been shown that the herringbones strongly depend on the faceting of the step. In this paper, we investigate the influence of terrace width on the herringbone pattern. STM investigations are first presented and then compared to molecular statics simulations using a modified embedded atom method (MEAM) interatomic potential.

II. EXPERIMENTAL RESULTS

Gold crystals were prepared by cycles of ion sputtering (Ar, 0.9 keV, 15 min) and annealing (20 min, 580°C) in an ultra-high-vacuum (UHV) environment with a base pressure of 3×10^{-11} mbar [24] to obtain a crystalline surface of good quality for STM investigations. Figure 1(a) shows a characteristic STM image performed at 300 K. Vicinal steps with $\{100\}$ microfacets [2,23] are mainly observed here lying along the $[1\bar{1}0]$ direction, with an atomic height of approximately 240 pm. As expected, herringbones are observed on large terraces [see at bottom left in Fig. 1(a)], with SPDs (white lines) oriented along the $\langle 112 \rangle$ directions. Average values for the fcc and hcp periodicity λ and for the height of SPDs are equal to 6.50 ± 0.20 nm and 20 ± 5 pm, respectively, in agreement with literature [2]. The reconstructed pattern is sometimes more simple with only one orientation of the SPDs [see inside the white dashed frame in Fig. 1(a)]. In this case, SPDs stay perpendicular to the step edge on its right side (upper terrace) while U-shape SPDs are observed on its left side (lower terrace). As already described [13,15], the U-shape SPD exhibits a threading edge dislocation at its apex that corresponds to the constriction of the two Shockley partial dislocations. Finally, on the lower terrace, another partial Shockley dislocation is lying between the U-shape SPDs and the step, parallel to the latter [Fig. 1(b)]. The width of the hcp-stacked area is smaller than that of the fcc area, so that the area inside the U turn corresponds to the fcc [20]. Figure 1(a) shows that λ depends on the width of the terrace. This behavior was confirmed in Fig. 1(c) where a terrace exhibiting a continuously decreasing width is observed with respect to the SPDs. Figure 2 shows both λ and the hcp width d of the SPDs, as a function of the terrace width L . It is shown that λ increases with the decreasing width L . It is emphasized that such a behavior has been already mentioned by Repain *et al.* [23]. For large terrace widths, the expected value of $\lambda = 6.50$ nm is superimposed in Fig. 2(a) as a horizontal dashed line. It supports the idea that the vicinal steps do not play any role at such a distance. In addition, whatever the terrace width L , d is shown to stay constant

^{*}julien.durinck@univ-poitiers.fr

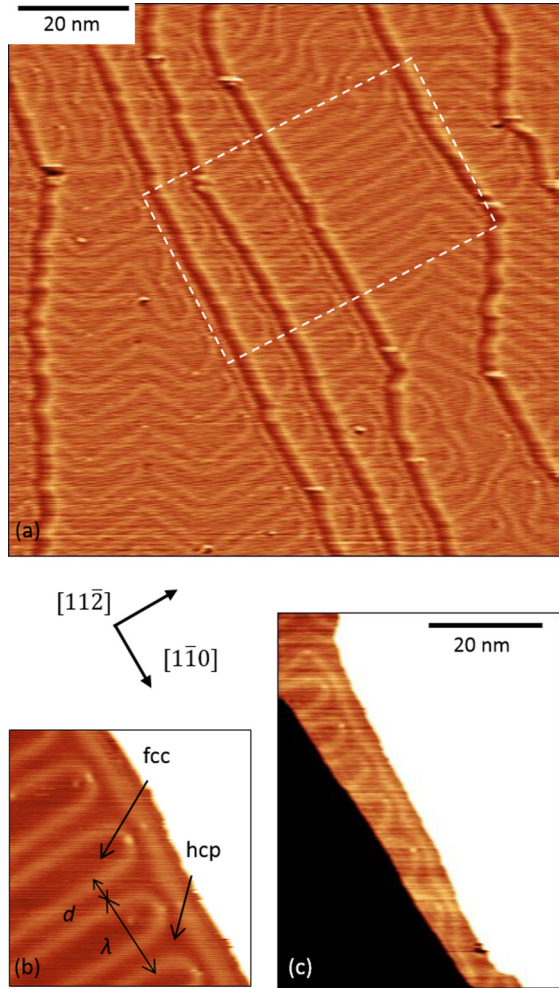


FIG. 1. STM images of Au(111) at room temperature. (a) Overview of the herringbones. (b) Details of the fcc/hcp areas closed to a vicinal step with a $\{100\}$ microfacet. (c) Herringbones on a terrace exhibiting a continuous decreasing width.

[Fig. 2(b)]. As a result, only the fcc area is increased while the terrace width is decreased. Hereafter, atomistic simulations using interatomic potentials are presented to firmly assess the origin of the observed behavior.

III. SIMULATION AND DISCUSSION

A gold fcc single crystal with a (111) stepped free surface was built by repeating in space n_u , n_v , and n_w times the two atoms hexagonal unit cell along the basis vectors $\vec{u} = \frac{a_0}{2}[\bar{1}\bar{1}0]$, $\vec{v} = \frac{a_0}{2}[11\bar{2}]$, and $\vec{w} = \frac{a_0}{2}[011]$, respectively, with a_0 the lattice parameter. A triclinic simulation cell with periodic boundary conditions has been considered with the axes $\vec{L}_x = n_u\vec{u}$, $\vec{L}_y = n_v\vec{v} + \vec{w}$, and $\vec{L}_z = (n_w + n_{\text{vac}})\vec{w}$, where n_{vac} is the thickness of vacuum in the (111) plane spacing unit [see Fig. 3(a)]. It leads to vicinal surfaces exhibiting monoatomic steps with $\{100\}$ facets, lying along the $[110]$ direction and spaced from each other by $L = n_v a_0 \sqrt{6}/2$. The configuration of the simulation cell is shown Fig. 3(b). A perfect edge dislocation with a $1/2[\bar{1}\bar{1}0]$ Burgers vector and a line extending along

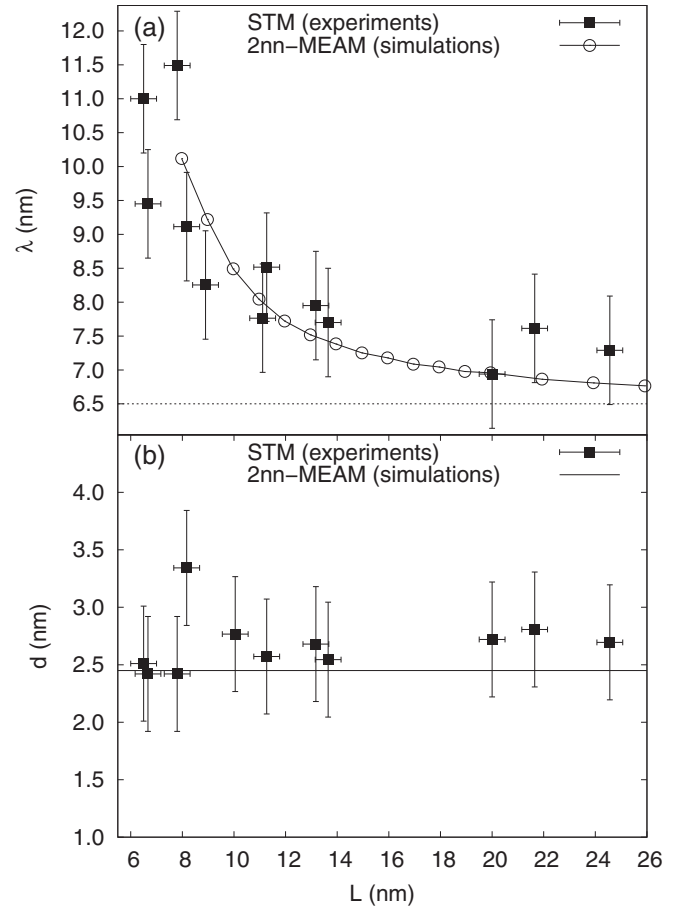


FIG. 2. Geometrical parameters of the surface reconstruction measured by STM and determined by atomistic simulations. (a) Periodicity λ and (b) hcp width d of the U-shape SPDs vs terrace width L .

$[11\bar{2}]$ from one step to a distance t from the other has been introduced. The relaxation procedure leads to its dissociation into two Shockley partials, with $1/6[\bar{2}11]$ and $1/6[\bar{1}\bar{2}\bar{1}]$ Burgers vectors, connected together at the constriction point by a threading $1/2[\bar{1}\bar{1}0]$, which corresponds to the U shape experimentally observed. The periodicity λ of the U shape is equal to $n_u a_0 \sqrt{2}/2$. The model also includes a $1/6[11\bar{2}]$ edge Shockley partial parallel to the step, between the U turns and the ascending step, to mimic the experimental observations.

The second-nearest neighbor modified embedded atom method (2nn-MEAM) parametrization of Lee *et al.* [25] has been considered as a starting point. The improvement brought by Ryu *et al.* [26] has also been implemented in order to unscreen the 2nn interactions. Finally, three other parameters have been adjusted so that the 2nn-MEAM potential accurately describes the Au(111) reconstruction, i.e., the $(22 \times \sqrt{3})$ reconstruction (see Ref. [27]).

All simulations have been performed with $n_w = 20$ atomic layers in thickness and $n_{\text{vac}} = 6$. This is thick enough to prevent one free surface from interacting with the image of the other. Energy is minimized using a conjugate gradient algorithm to relax atomic positions until the force on each atom is lower than 10^{-5} eV/Å. Different values of the distance L ranging

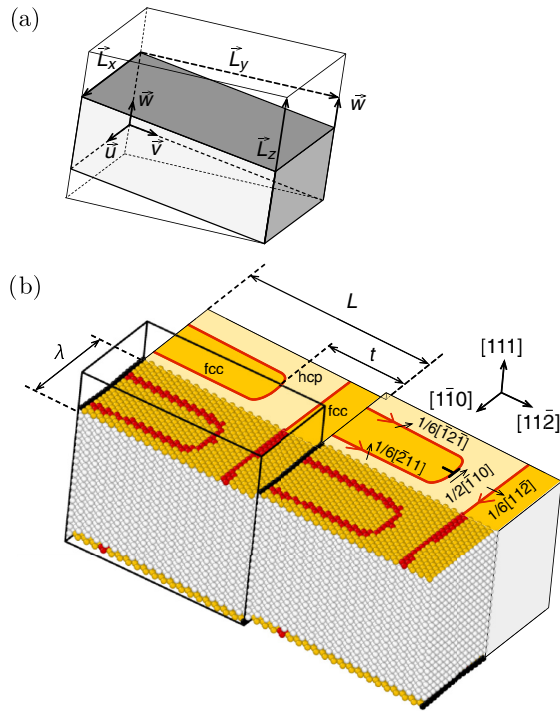


FIG. 3. (a) Configuration of the simulation cell and geometrical parameters used in the text, with $\vec{u} = \frac{a_0}{2} [1\bar{1}0]$, $\vec{v} = \frac{a_0}{2} [11\bar{2}]$, and $\vec{w} = \frac{a_0}{2} [011]$. (b) Relaxed configuration of the stepped surface after energy minimization and schematic description of the surface reconstruction in terms of misfit dislocations. Atoms are colored according to the number of first neighboring atoms: light gray is for atoms in bulk fcc crystal, orange is for atoms at free (111) surfaces, black is for atoms located at surface steps, and red is for atoms belonging to dislocation lines.

from 8 to 26 nm have been considered. The optimum value of λ minimizing the system energy has been determined as a function of L , with $t = 4$ nm. It has been checked that other values of t lead to higher system energies. The evolutions of the optimum λ and the width d of the hcp region are superimposed in Figs. 2(a) and 2(b), respectively. It shows that λ decreases as the width L of the terrace increases, with the same range as in STM observations. d is found constant and equal to 2.45 nm, also in agreement with the average value of 2.7 nm measured by STM.

The surface stress of the nonreconstructed surface has been calculated as a function of the step-to-step distance L . The same simulation geometry has been considered with $n_u = 4$, $n_w = 20$, and $n_{vac} = 6$. The surface stress τ_{ii} is defined as

$$\tau_{ii} = \frac{1}{S_0} \left(\frac{\partial E_{\text{surf}}(\varepsilon_{ii})}{\partial \varepsilon_{ii}} \right)_{\varepsilon_{ii}=0}, \quad (1)$$

where ε_{ii} are the diagonal components of the 2×2 strain tensor with $i = x$ or y , $S_0 = L_x \times L_y^0$ is the projected area of the vicinal surface on the (111) surface for $\varepsilon_{ii} = 0$ with $L_y^0 = L - \frac{\sqrt{6}}{12} a_0$, and $E_{\text{surf}} = (E_{\text{tot}} - N E_{\text{bulk}})/2$ is the excess energy due to the surface, with N the number of atoms, E_{tot} the total energy of the considered system, and E_{bulk} the energy of an atom in the bulk Au crystal. Several values of the strains

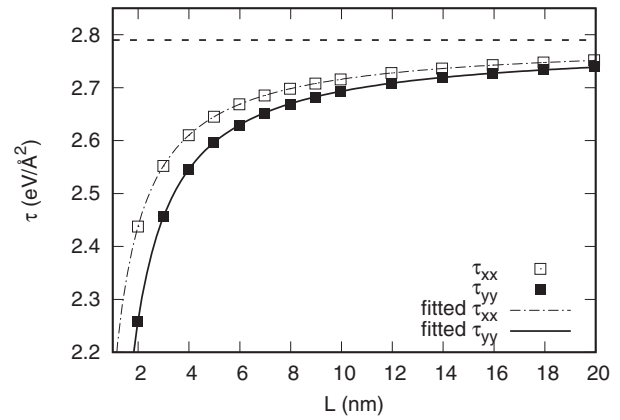


FIG. 4. Evolution of the surface stresses τ_{xx} and τ_{yy} with respect to the distance L between steps.

ε_{ii} ranging in $[-0.003, 0.003]$ have been used to derive the surface stress from Eq. (1). The resulting evolutions of τ_{xx} and τ_{yy} have been plotted in Fig. 4 with respect to L . It is shown that, when L is large, both τ_{xx} and τ_{yy} tend towards 2.79 J/m^2 , the value of the nonstepped surface stress. τ_{xx} and τ_{yy} stay in tension and decrease with decreasing L . It supports the idea that the width dependence of the SPD periodicity comes from the release of the tensile surface stress τ_{xx} parallel to the step.

τ_{ii} can be considered as the sum of three contributions, written according to Salanon and Hecquet [28], as

$$\tau_{ii} = \tau_{ii}^0 + \frac{\beta_{ii}}{L_y^0} + \Gamma_{ii} \frac{h^2}{L_y^0}, \quad (2)$$

where h is the distance between two adjacent (111) atomic planes, τ_{ii}^0 is the nonstepped (111) surface stress, and β_{ii} and Γ_{ii} stand for the step contribution and the step-step interaction, respectively. The calculated values of τ_{xx} and τ_{yy} have been fitted using Eq. (2) (see Fig. 4). It is found that (i) $\tau_{xx}^0 = \tau_{yy}^0 = 2.79 \text{ eV/\AA}^2$, in agreement with the value computed directly for systems with no steps on the (111) surface; (ii) $\beta_{xx} = -0.72 \text{ eV/\AA}$ and $\beta_{yy} = -0.85 \text{ eV/\AA}$, meaning that steps reduce the tensile surface stress; and (iii) $\Gamma_{xx} = 0.02 \text{ eV/\AA}^2$ and $\Gamma_{yy} = -0.05 \text{ eV/\AA}^2$, which are negligible in comparison to the two other contributions. The release of the tensile surface stresses is more pronounced when the terrace width is decreased, due to the increase of the step contribution [second term defined in Eq. (2)].

The tensor $\Delta \varepsilon$ of the strain variation induced by the step has been determined from the comparison of two relaxed configurations without and with a surface step, using the atomistic visualization software OVITO [29]. It is found that only the three components $\Delta \varepsilon_{yy}$, $\Delta \varepsilon_{yz}$, and $\Delta \varepsilon_{zz}$ are not equal to zero (Fig. 5) and are maximum in magnitude at the top surface layer, on the upper side of the step. It shows that the step not only induces an out-of-plane strain variation $\Delta \varepsilon_{zz}$ (as already proposed by Li *et al.* [30]) but also in-plane strain variations $\Delta \varepsilon_{yy}$ and $\Delta \varepsilon_{yz}$ close to the step.

The component $\Delta \varepsilon_{yy}$ is mainly responsible for the relaxation of τ_{yy} , but also for the relaxation of τ_{xx} through a transverse elastic coupling. The transverse elastic response to the strain variation $\Delta \varepsilon_{zz}$ and in-plane shear relaxation $\Delta \varepsilon_{yz}$

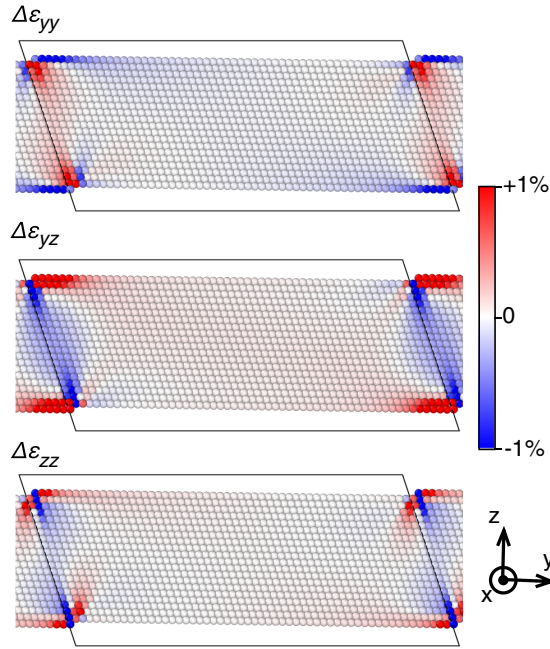


FIG. 5. Distribution of the strain variation $\Delta\epsilon_{yy}$, $\Delta\epsilon_{yz}$, and $\Delta\epsilon_{zz}$ induced by a vicinal step, for $L = 14$ nm.

may also play a role in surface stress relaxation, as it was suggested by Li *et al.* [30].

IV. CONCLUSION

It has been experimentally shown that the periodicity of the SPDs at the free surface of Au(111) single crystals is significantly modified by vicinal steps. It particularly depends on the width of the resulting terraces already mentioned in [23]. The present atomistic simulations have quantitatively demonstrated that this behavior is explained by the release of the tensile surface stresses, both along and perpendicular to the vicinal steps. It is believed that these results will give insights on how to find new ways to pattern surfaces at the atomic scale by a nanomechanical engineering approach.

ACKNOWLEDGMENTS

This work was partially funded by the French Government program Investissements d' Avenir (LABEX INTERACTIFS Grant No. ANR-11-LABX-0017-01). The authors thank the Alphatrad society for the English polishing.

- [1] C. Wöll, S. Chiang, R. J. Wilson, and P. H. Lippel, *Phys. Rev. B* **39**, 7988 (1989).
- [2] V. Repain, J. M. Berroir, S. Rousset, and J. Lecoer, *App. Surf. Sci.* **162**, 30 (2000).
- [3] J. V. Barth, H. Brune, G. Ertl, and R. J. Behm, *Phys. Rev. B* **42**, 9307 (1990).
- [4] K. G. Huang, D. Gibbs, D. M. Zehner, A. R. Sandy, and S. G. J. Mochrie, *Phys. Rev. Lett.* **65**, 3313 (1990).
- [5] L. D. Marks, V. Heine, and D. J. Smith, *Phys. Rev. Lett.* **52**, 656 (1984).
- [6] Y. Tanishiro, H. Kanamori, K. Takayanagi, K. Yagi, and G. Honjo, *Surf. Sci.* **111**, 395 (1981).
- [7] U. Harten, A. M. Lahee, J. P. Toennies, and C. Wöll, *Phys. Rev. Lett.* **54**, 2619 (1985).
- [8] O. Ourdjini, R. Pawlak, M. Abel, S. Clair, L. Chen, N. Bergeon, M. Sassi, V. Oison, J. M. Debierre, R. Coratger, and L. Porte, *Phys. Rev. B* **84**, 125421 (2011).
- [9] C. S. Casari, S. Foglio, F. Siviero, A. Li Bassi, M. Passoni, and C. E. Bottani, *Phys. Rev. B* **79**, 195402 (2009).
- [10] O. Fruchart, M. Klaua, J. Barthel, and J. Kirschner, *Phys. Rev. Lett.* **83**, 2769 (1999).
- [11] M. Corso, L. Fernández, F. Schiller, and J. E. Ortega, *ACS Nano* **4**, 1603 (2010).
- [12] M. M. Biener, J. Biener, R. Schalek, and C. M. Friend, *Surf. Sci.* **594**, 221 (2005).
- [13] C. B. Carter and R. Q. Hwang, *Phys. Rev. B* **51**, 4730 (1995).
- [14] O. Schaff, A. Schmid, N. Bartelt, J. de la Figuera, and R. Hwang, *Mat. Sci. Eng. A* **319**, 914 (2001).
- [15] A. K. Schmid, N. C. Bartelt, J. C. Hamilton, C. B. Carter, and R. Q. Hwang, *Phys. Rev. Lett.* **78**, 3507 (1997).
- [16] N. Takeuchi, C. T. Chan, and K. M. Ho, *Phys. Rev. B* **43**, 13899 (1991).
- [17] S. Narasimhan and D. Vanderbilt, *Phys. Rev. Lett.* **69**, 1564 (1992).
- [18] C. E. Bach, M. Giesen, H. Ibach, and T. L. Einstein, *Phys. Rev. Lett.* **78**, 4225 (1997).
- [19] H. Bulou and C. Goyhenex, *Phys. Rev. B* **65**, 045407 (2002).
- [20] Y. Wang, N. S. Hush, and J. R. Reimers, *Phys. Rev. B* **75**, 233416 (2007).
- [21] U. Tartaglino, E. Tosatti, D. Passerone, and F. Ercolessi, *Phys. Rev. B* **65**, 241406(R) (2002).
- [22] C. Coupeau, O. Camara, M. Drouet, J. Durinck, J. Bonneville, J. Colin, and J. Grilhé, *Phys. Rev. B* **93**, 041405(R) (2016).
- [23] V. Repain, J. M. Berroir, S. Rousset, and J. Lecoer, *Europhys. Lett.* **47**, 435 (1999).
- [24] Y. Nahas, F. Berneau, J. Bonneville, C. Coupeau, M. Drouet, B. Lamongie, M. Marteau, J. Michel, P. Tanguy, and C. Tromas, *Rev. Sci. Instrum.* **84**, 105117 (2013).
- [25] B.-J. Lee, J.-H. Shim, and M. I. Baskes, *Phys. Rev. B* **68**, 144112 (2003).
- [26] S. Ryu, C. R. Weinberger, M. I. Baskes, and W. Cai, *Model. Simul. Mater. Sc.* **17**, 075008 (2009).
- [27] See Supplemental Material at <http://link.aps.org/supplemental/10.1103/PhysRevB.96.045410> for the MEAM potential parametrization.
- [28] B. Salanon and P. Hecquet, *Surf. Sci.* **412**, 639 (1998).
- [29] A. Stukowski, *Model. Simul. Mater. Sc.* **18**, 015012 (2010).
- [30] W. Li, H. Duan, K. Albe, and J. Weissmüller, *Surf. Sci.* **605**, 947 (2011).